Measurement of b hadron masses in exclusive J/ψ decays with the CDF detector

D. Acosta,[16] J. Adelman,[12] T. Affolder,[9] T. Akimoto,[54] M.G. Albrow,[15] D. Ambrose,[15] S. Amerio,[42] D. Amidei,[33] A. Anastassov,[50] K. Anikeev,[15] A. Annovi,[44] J. Antos,[1] M. Aoki,[54] G. Apollinari,[15] T. Arisawa,[56] J-F. Arguin,[32] A. Artikov,[13] W. Ashmanskas,[15] A. Attal,[7] F. Azfar,[41] P. Azzi-Bacchetta,[42] N. Bacchetta,[42] H. Bachacou,[28] W. Badgett,[15] A. Barbaro-Galtieri,[28] G.J. Barker,[25] V.E. Barnes,[46] B.A. Barnett,[24] S. Baroiant,[6] G. Bauer,[31] F. Bedeschi,[44] S. Behari,[24] S. Belforte,[53] G. Bellettini,[44] J. Bellinger,[58] A. Belloni,[31] E. Ben-Haim,[15] D. Benjamin,[14] A. Beretvas,[15] T. Berry,[29] A. Bhatti,[48] M. Binkley,[15] D. Bisello,[42] M. Bishai,[15] R.E. Blair,[2] C. Blocker,[5] K. Bloom,[33] B. Blumenfeld,[24] A. Bocci,[48] A. Bodek,[47] G. Bolla,[46] A. Bolshov,[31] D. Bortoletto,[46] J. Boudreau,[45] S. Bourov,[15] B. Brau,[9] C. Bromberg,[34] E. Brubaker,[12] J. Budagov,[13] H.S. Budd,[47] K. Burkett,[15] G. Busetto,[42] P. Bussey,[19] K.L. Byrum,[2] S. Cabrera,[14] M. Campanelli,[18] M. Campbell,[33] F. Canelli,[7] A. Canepa,[46] M. Casarsa,[53] D. Carlsmith,[58] R. Carosi,[44] S. Carron,[14] M. Cavalli-Sforza,[3] A. Castro,[4] P. Catastini,[44] D. Cauz,[53] A. Cerri,[28] L. Cerrito,[41] J. Chapman,[33] Y.C. Chen,[1] M. Chertok,[6] G. Chiarelli,[44] G. Chlachidze,[13] F. Chlebana,[15] I. Cho,[27] K. Cho,[27] D. Chokheli,[13] J.P. Chou,[20] S. Chuang,[58] K. Chung,[11] W-H. Chung,[58] Y.S. Chung,[47] M. Cijliak,[44] C.I. Ciobanu,[23] M.A. Ciocci,[44] A.G. Clark,[18] D. Clark,[5] M. Coca,[14] A. Connolly,[28] M. Convery,[48] J. Conway,[6] B. Cooper,[30] K. Copic,[33] M. Cordelli,[17] G. Cortiana,[42] J. Cranshaw,[52] J. Cuevas,[10] A. Cruz,[16] R. Culbertson,[15] C. Currat,[28] D. Cyr,[58] D. Dagenhart,[5] S. Da Ronco,[42] S. D'Auria,[19] P. de Barbaro,[47] S. De Cecco,[49] A. Deisher,[28] G. De Lentdecker,[47] M. Dell'Orso,[44] S. Demers,[47] L. Demortier,[48] M. Deninno,[4] D. De Pedis,[49] P.F. Derwent,[15] C. Dionisi,[49] J.R. Dittmann,[15] P. DiTuro,[50] C. Dörr,[25] A. Dominguez,[28] S. Donati,[44] M. Donega,[18] J. Donini,[42] M. D'Onofrio,[18] T. Dorigo,[42] K. Ebina,[56] J. Efron,[38] J. Ehlers,[18] R. Erbacher,[6] M. Erdmann,[25] D. Errede,[23] S. Errede,[23] R. Eusebi,[47] H-C. Fang,[28] S. Farrington,[29] I. Fedorko,[44] W.T. Fedorko,[12] R.G. Feild,[59] M. Feindt,[25] J.P. Fernandez,[46] R.D. Field,[16] G. Flanagan,[34] L.R. Flores-Castillo,[45] A. Foland,[20] S. Forrester,[6] G.W. Foster,[15] M. Franklin,[20] J.C. Freeman,[28] Y. Fujii,[26] I. Furic,[12] A. Gajjar,[29] M. Gallinaro,[48] J. Galyardt,[11] M. Garcia-Sciveres,[28] A.F. Garfinkel,[46] C. Gay,[59] H. Gerberich,[14] D.W. Gerdes,[33] E. Gerchtein,[11] S. Giagu,[49] P. Giannetti,[44] A. Gibson,[28] K. Gibson,[11] C. Ginsburg,[15] K. Giolo,[46] M. Giordani,[53] M. Giunta,[44] G. Giurgiu,[11] V. Glagolev,[13] D. Glenzinski,[15] M. Gold,[36] N. Goldschmidt,[33] D. Goldstein,[7] J. Goldstein,[41] G. Gomez,[10] G. Gomez-Ceballos,[10] M. Goncharov,[51] O. González,[46] I. Gorelov,[36] A.T. Goshaw,[14] Y. Gotra,[45] K. Goulianos,[48] A. Gresele,[42] M. Griffiths,[29] C. Grosso-Pilcher,[12] U. Grundler,[23] J. Guimaraes da Costa,[20] C. Haber,[28] K. Hahn,[43] S.R. Hahn,[15] E. Halkiadakis,[47] A. Hamilton,[32] B-Y. Han,[47] R. Handler,[58] F. Happacher,[17] K. Hara,[54] M. Hare,[55] R.F. Harr,[57] R.M. Harris,[15] F. Hartmann,[25] K. Hatakeyama,[48] J. Hauser,[7] C. Hays,[14] H. Hayward,[29] B. Heinemann,[29] J. Heinrich,[43] M. Hennecke,[25] M. Herndon,[24] C. Hill,[9] D. Hirschbuehl,[25] A. Hocker,[15] K.D. Hoffman,[12] A. Holloway,[20] S. Hou,[1] M.A. Houlden,[29] B.T. Huffman,[41] Y. Huang,[14] R.E. Hughes,[38] J. Huston,[34] K. Ikado,[56] J. Incandela,[9] G. Introzzi,[44] M. Iori,[49] Y. Ishizawa,[54] C. Issever,[9] A. Ivanov,[6] Y. Iwata,[22] B. Iyutin,[31] E. James,[15] D. Jang,[50] B. Jayatilaka,[33] D. Jeans,[49] H. Jensen,[15] E.J. Jeon,[27] M. Jones,[46] K.K. Joo,[27] S.Y. Jun,[11] T. Junk,[23] T. Kamon,[51] J. Kang,[33] M. Karagoz Unel,[37] P.E. Karchin,[57] Y. Kato,[40] Y. Kemp,[25] R. Kephart,[15] U. Kerzel,[25] V. Khotilovich,[51] B. Kilminster,[38] D.H. Kim,[27] H.S. Kim,[23] J.E. Kim,[27] M.J. Kim,[11] M.S. Kim,[27] S.B. Kim,[27] S.H. Kim,[54] Y.K. Kim,[12] M. Kirby,[14] L. Kirsch,[5] S. Klimenko,[16] M. Klute,[31] B. Knuteson,[31] B.R. Ko,[14] H. Kobayashi,[54] D.J. Kong,[27] K. Kondo,[56] J. Konigsberg,[16] K. Kordas,[32] A. Korn,[31] A. Korytov,[16] A.V. Kotwal,[14] A. Kovalev,[43] J. Kraus,[23] I. Kravchenko,[31] A. Kreymer,[15] J. Kroll,[43] M. Kruse,[14] V. Krutelyov,[51] S.E. Kuhlmann,[2] S. Kwang,[12] A.T. Laasanen,[46] S. Lai,[32] S. Lami,[44] S. Lammel,[15] M. Lancaster,[30] R. Lander,[6] K. Lannon,[38] A. Lath,[50] G. Latino,[44] I. Lazzizzera,[42] C. Lecci,[25] T. LeCompte,[2] J. Lee,[27] J. Lee,[47] S.W. Lee,[51] R. Lefèvre,[3] N. Leonardo,[31] S. Leone,[44] S. Levy,[12] J.D. Lewis,[15] K. Li,[59] C. Lin,[59] C.S. Lin,[15] M. Lindgren,[15] E. Lipeles,[8] T.M. Liss,[23] A. Lister,[18] D.O. Litvintsev,[15] T. Liu,[15] Y. Liu,[18] N.S. Lockyer,[43] A. Loginov,[35] M. Loreti,[42] P. Loverre,[49] R-S. Lu,[1] D. Lucchesi,[42] P. Lujan,[28] P. Lukens,[15] G. Lungu,[16] L. Lyons,[41] J. Lys,[28] R. Lysak,[1] E. Lytken,[46] D. MacQueen,[32] R. Madrak,[15] K. Maeshima,[15] P. Maksimovic,[24] G. Manca,[29] F. Margaroli,[4] R. Marginean,[15] C. Marino,[23] A. Martin,[59] M. Martin,[24] V. Martin,[37] M. Martínez,[3] T. Maruyama,[54] H. Matsunaga,[54] M. Mattson,[57] P. Mazzanti,[4] K.S. McFarland,[47] D. McGivern,[30] P.M. McIntyre,[51] P. McNamara,[50] R. McNulty,[29] A. Mehta,[29] S. Menzemer,[31] A. Menzione,[44] P. Merkel,[46] C. Mesropian,[48] A. Messina,[49] T. Miao,[15] N. Miladinovic,[5] J. Miles,[31] L. Miller,[20] R. Miller,[34] J.S. Miller,[33] C. Mills,[9] R. Miquel,[28] S. Miscetti,[17] G. Mitselmakher,[16] A. Miyamoto,[26] N. Moggi,[4] B. Mohr,[7] R. Moore,[15] M. Morello,[44] P.A. Movilla Fernandez,[28] J. Muelmenstaedt,[28] A. Mukherjee,[15] M. Mulhearn,[31] T. Muller,[25] R. Mumford,[24] A. Munar,[43] P. Murat,[15] J. Nachtman,[15] S. Nahn,[59] I. Nakano,[39] A. Napier,[55] R. Napora,[24] D. Naumov,[36] V. Necula,[16] J. Nielsen,[28]

T. Nelson,[15] C. Neu,[43] M.S. Neubauer,[8] T. Nigmanov,[45] L. Nodulman,[2] O. Norniella,[3] T. Ogawa,[56] S.H. Oh,[14] Y.D. Oh,[27] T. Ohsugi,[22] T. Okusawa,[40] R. Oldeman,[29] R. Orava,[21] W. Orejudos,[28] K. Osterberg,[21] C. Pagliarone,[44] E. Palencia,[10] R. Paoletti,[44] V. Papadimitriou,[15] A.A. Paramonov,[12] S. Pashapour,[32] J. Patrick,[15] G. Pauletta,[53] M. Paulini,[11] C. Paus,[31] D. Pellett,[6] A. Penzo,[53] T.J. Phillips,[14] G. Piacentino,[44] J. Piedra,[10] K.T. Pitts,[23] C. Plager,[7] L. Pondrom,[58] G. Pope,[45] X. Portell,[3] O. Poukhov,[13] N. Pounder,[41] F. Prakoshyn,[13] A. Pronko,[16] J. Proudfoot,[2] F. Ptohos,[17] G. Punzi,[44] J. Rademacker,[41] M.A. Rahaman,[45] A. Rakitine,[31] S. Rappoccio,[20] F. Ratnikov,[50] H. Ray,[33] B. Reisert,[15] V. Rekovic,[36] P. Renton,[41] M. Rescigno,[49] F. Rimondi,[4] K. Rinnert,[25] L. Ristori,[44] W.J. Robertson,[14] A. Robson,[19] T. Rodrigo,[10] S. Rolli,[55] R. Roser,[15] R. Rossin,[16] C. Rott,[46] J. Russ,[11] V. Rusu,[12] A. Ruiz,[10] D. Ryan,[55] H. Saarikko,[21] S. Sabik,[32] A. Safonov,[6] R. St. Denis,[19] W.K. Sakumoto,[47] G. Salamanna,[49] D. Saltzberg,[7] C. Sanchez,[3] L. Santi,[53] S. Sarkar,[49] K. Sato,[54] P. Savard,[32] A. Savoy-Navarro,[15] P. Schlabach,[15] E.E. Schmidt,[15] M.P. Schmidt,[59] M. Schmitt,[37] T. Schwarz,[33] L. Scodellaro,[10] A.L. Scott,[9] A. Scribano,[44] F. Scuri,[44] A. Sedov,[46] S. Seidel,[36] Y. Seiya,[40] A. Semenov,[13] F. Semeria,[4] L. Sexton-Kennedy,[15] I. Sfiligoi,[17] M.D. Shapiro,[28] T. Shears,[29] P.F. Shepard,[45] D. Sherman,[20] M. Shimojima,[54] M. Shochet,[12] Y. Shon,[58] I. Shreyber,[35] A. Sidoti,[44] A. Sill,[52] P. Sinervo,[32] A. Sisakyan,[13] J. Sjolin,[41] A. Skiba,[25] A.J. Slaughter,[15] K. Sliwa,[55] D. Smirnov,[36] J.R. Smith,[6] F.D. Snider,[15] R. Snihur,[32] M. Soderberg,[33] A. Soha,[6] S.V. Somalwar,[50] J. Spalding,[15] M. Spezziga,[52] F. Spinella,[44] P. Squillacioti,[44] H. Stadie,[25] M. Stanitzki,[59] B. Stelzer,[32] O. Stelzer-Chilton,[32] D. Stentz,[37] J. Strologas,[36] D. Stuart,[9] J. S. Suh,[27] A. Sukhanov,[16] K. Sumorok,[31] H. Sun,[55] T. Suzuki,[54] A. Taffard,[23] R. Tafirout,[32] H. Takano,[54] R. Takashima,[39] Y. Takeuchi,[54] K. Takikawa,[54] M. Tanaka,[2] R. Tanaka,[39] N. Tanimoto,[39] M. Tecchio,[33] P.K. Teng,[1] K. Terashi,[48] R.J. Tesarek,[15] S. Tether,[31] J. Thom,[15] A.S. Thompson,[19] E. Thomson,[43] P. Tipton,[47] V. Tiwari,[11] S. Tkaczyk,[15] D. Toback,[51] K. Tollefson,[34] T. Tomura,[54] D. Tonelli,[44] M. Tönnesmann,[34] S. Torre,[44] D. Torretta,[15] W. Trischuk,[32] R. Tsuchiya,[56] S. Tsuno,[39] D. Tsybychev,[16] N. Turini,[44] F. Ukegawa,[54] T. Unverhau,[19] S. Uozumi,[54] D. Usynin,[43] L. Vacavant,[28] A. Vaiciulis,[47] A. Varganov,[33] S. Vejcik III,[15] G. Velev,[15] V. Veszpremi,[46] G. Veramendi,[23] T. Vickey,[23] R. Vidal,[15] I. Vila,[10] R. Vilar,[10] I. Vollrath,[32] I. Volobouev,[28] M. von der Mey,[7] P. Wagner,[51] R.G. Wagner,[2] R.L. Wagner,[15] W. Wagner,[25] R. Wallny,[7] T. Walter,[25] Z. Wan,[50] M.J. Wang,[1] S.M. Wang,[16] A. Warburton,[32] B. Ward,[19] S. Waschke,[19] D. Waters,[30] T. Watts,[50] M. Weber,[28] W.C. Wester III,[15] B. Whitehouse,[55] D. Whiteson,[43] A.B. Wicklund,[2] E. Wicklund,[15] H.H. Williams,[43] P. Wilson,[15] B.L. Winer,[38] P. Wittich,[43] S. Wolbers,[15] C. Wolfe,[12] M. Wolter,[55] M. Worcester,[7] S. Worm,[50] T. Wright,[33] X. Wu,[18] F. Würthwein,[8] A. Wyatt,[30] A. Yagil,[15] T. Yamashita,[39] K. Yamamoto,[40] J. Yamaoka,[50] C. Yang,[59] U.K. Yang,[12] W. Yao,[28] G.P. Yeh,[15] J. Yoh,[15] K. Yorita,[56] T. Yoshida,[40] I. Yu,[27] S. Yu,[43] J.C. Yun,[15] L. Zanello,[49] A. Zanetti,[53] I. Zaw,[20] F. Zetti,[44] J. Zhou,[50] and S. Zucchelli[4]

(CDF Collaboration)

[1]*Institute of Physics, Academia Sinica, Taipei, Taiwan 11529, Republic of China*
[2]*Argonne National Laboratory, Argonne, Illinois 60439*
[3]*Institut de Fisica d'Altes Energies, Universitat Autonoma de Barcelona, E-08193, Bellaterra (Barcelona), Spain*
[4]*Istituto Nazionale di Fisica Nucleare, University of Bologna, I-40127 Bologna, Italy*
[5]*Brandeis University, Waltham, Massachusetts 02254*
[6]*University of California, Davis, Davis, California 95616*
[7]*University of California, Los Angeles, Los Angeles, California 90024*
[8]*University of California, San Diego, La Jolla, California 92093*
[9]*University of California, Santa Barbara, Santa Barbara, California 93106*
[10]*Instituto de Fisica de Cantabria, CSIC-University of Cantabria, 39005 Santander, Spain*
[11]*Carnegie Mellon University, Pittsburgh, PA 15213*
[12]*Enrico Fermi Institute, University of Chicago, Chicago, Illinois 60637*
[13]*Joint Institute for Nuclear Research, RU-141980 Dubna, Russia*
[14]*Duke University, Durham, North Carolina 27708*
[15]*Fermi National Accelerator Laboratory, Batavia, Illinois 60510*
[16]*University of Florida, Gainesville, Florida 32611*
[17]*Laboratori Nazionali di Frascati, Istituto Nazionale di Fisica Nucleare, I-00044 Frascati, Italy*
[18]*University of Geneva, CH-1211 Geneva 4, Switzerland*
[19]*Glasgow University, Glasgow G12 8QQ, United Kingdom*
[20]*Harvard University, Cambridge, Massachusetts 02138*
[21]*Division of High Energy Physics, Department of Physics,*
University of Helsinki and Helsinki Institute of Physics, FIN-00014, Helsinki, Finland
[22]*Hiroshima University, Higashi-Hiroshima 724, Japan*
[23]*University of Illinois, Urbana, Illinois 61801*
[24]*The Johns Hopkins University, Baltimore, Maryland 21218*

[25] *Institut für Experimentelle Kernphysik, Universität Karlsruhe, 76128 Karlsruhe, Germany*
[26] *High Energy Accelerator Research Organization (KEK), Tsukuba, Ibaraki 305, Japan*
[27] *Center for High Energy Physics: Kyungpook National University, Taegu 702-701; Seoul National University, Seoul 151-742; and SungKyunKwan University, Suwon 440-746; Korea*
[28] *Ernest Orlando Lawrence Berkeley National Laboratory, Berkeley, California 94720*
[29] *University of Liverpool, Liverpool L69 7ZE, United Kingdom*
[30] *University College London, London WC1E 6BT, United Kingdom*
[31] *Massachusetts Institute of Technology, Cambridge, Massachusetts 02139*
[32] *Institute of Particle Physics: McGill University, Montréal, Canada H3A 2T8; and University of Toronto, Toronto, Canada M5S 1A7*
[33] *University of Michigan, Ann Arbor, Michigan 48109*
[34] *Michigan State University, East Lansing, Michigan 48824*
[35] *Institution for Theoretical and Experimental Physics, ITEP, Moscow 117259, Russia*
[36] *University of New Mexico, Albuquerque, New Mexico 87131*
[37] *Northwestern University, Evanston, Illinois 60208*
[38] *The Ohio State University, Columbus, Ohio 43210*
[39] *Okayama University, Okayama 700-8530, Japan*
[40] *Osaka City University, Osaka 588, Japan*
[41] *University of Oxford, Oxford OX1 3RH, United Kingdom*
[42] *University of Padova, Istituto Nazionale di Fisica Nucleare, Sezione di Padova-Trento, I-35131 Padova, Italy*
[43] *University of Pennsylvania, Philadelphia, Pennsylvania 19104*
[44] *Istituto Nazionale di Fisica Nucleare Pisa, Universities of Pisa, Siena and Scuola Normale Superiore, I-56127 Pisa, Italy*
[45] *University of Pittsburgh, Pittsburgh, Pennsylvania 15260*
[46] *Purdue University, West Lafayette, Indiana 47907*
[47] *University of Rochester, Rochester, New York 14627*
[48] *The Rockefeller University, New York, New York 10021*
[49] *Istituto Nazionale di Fisica Nucleare, Sezione di Roma 1, University di Roma "La Sapienza," I-00185 Roma, Italy*
[50] *Rutgers University, Piscataway, New Jersey 08855*
[51] *Texas A&M University, College Station, Texas 77843*
[52] *Texas Tech University, Lubbock, Texas 79409*
[53] *Istituto Nazionale di Fisica Nucleare, University of Trieste/ Udine, Italy*
[54] *University of Tsukuba, Tsukuba, Ibaraki 305, Japan*
[55] *Tufts University, Medford, Massachusetts 02155*
[56] *Waseda University, Tokyo 169, Japan*
[57] *Wayne State University, Detroit, Michigan 48201*
[58] *University of Wisconsin, Madison, Wisconsin 53706*
[59] *Yale University, New Haven, Connecticut 06520*
(Dated: February 5, 2008)

We measure the masses of b hadrons in exclusively reconstructed final states containing a $J/\psi \to \mu^- \mu^+$ decay using 220 pb^{-1} of data collected by the CDF II experiment. We find:

$$
\begin{aligned}
m(B^+) &= 5279.10 \pm 0.41 \,_{(stat.)} \pm 0.36 \,_{(sys.)} \text{ MeV}/c^2, \\
m(B^0) &= 5279.63 \pm 0.53 \,_{(stat.)} \pm 0.33 \,_{(sys.)} \text{ MeV}/c^2, \\
m(B^0_s) &= 5366.01 \pm 0.73 \,_{(stat.)} \pm 0.33 \,_{(sys.)} \text{ MeV}/c^2, \\
m(\Lambda^0_b) &= 5619.7 \pm 1.2 \,_{(stat.)} \pm 1.2 \,_{(sys.)} \text{ MeV}/c^2. \\
m(B^+) - m(B^0) &= -0.53 \pm 0.67 \,_{(stat.)} \pm 0.14 \,_{(sys.)} \text{ MeV}/c^2, \\
m(B^0_s) - m(B^0) &= 86.38 \pm 0.90 \,_{(stat.)} \pm 0.06 \,_{(sys.)} \text{ MeV}/c^2, \\
m(\Lambda^0_b) - m(B^0) &= 339.2 \pm 1.4 \,_{(stat.)} \pm 0.1 \,_{(sys.)} \text{ MeV}/c^2.
\end{aligned}
$$

The measurements of the B^0_s, Λ^0_b mass, $m(B^0_s) - m(B^0)$ and $m(\Lambda^0_b) - m(B^0)$ mass difference are of better precision than the current world averages.

In the Standard Model, Quantum Chromodynamics (QCD) is the theory describing strong interactions between objects of color charge [1]. Hadrons are colorless particles made up of strongly-interacting constituents.

Hadron masses are fundamental physical observables and their study is the spectroscopy of quark systems bound by QCD. The heaviest known hadrons contain a bottom or b quark [2]. Lattice QCD calculations predict the

hadron mass spectra from first principles. Comparing these calculations with experimental data is an essential test of QCD. Recent advances in lattice QCD, using unquenched methods, will soon allow mass predictions with close to the experimental accuracy [3] and we look forward to these new calculations to compare with our results. The most precise predictions are those of b hadron mass differences. We present here the most precise individual measurements, to date, for the masses of B^+, B^0, B_s^0 and Λ_b^0.

The data used in this analysis were obtained with the Collider Detector at Fermilab (CDF II) operating at the $\sqrt{s} = 1.96$ TeV Tevatron $p\bar{p}$-collider. The data were collected between February 2002 and August 2003 and corresponds to an integrated luminosity of 220 pb^{-1}. The CDF II detector is described in detail elsewhere [4]. This analysis relies on the tracking system and the muon detectors. The tracking system is comprised of a silicon micro strip vertex detector (SVX II) [5] and a drift chamber operating in a 1.4 T solenoidal magnetic field. The SVX II system consists of 5 concentric silicon layers made of double-sided silicon covering the radii from 2.5 cm to 10.6 cm. The impact parameter resolution is about 40 μm, including a 30 μm contribution from the beamspot. The Central Outer Tracker (COT) [6] is an open cell drift chamber measuring 310 cm in length, with an inner radius of 41 cm extending to a radius of 138 cm and provides a large lever arm for curvature measurements. Each cell contains a plane of 12 sense wires tilted by 35° with respect to the radial direction to compensate for the drift Lorentz-angle. The COT is segmented radially into eight superlayers. For superlayers 1, 3, 5 and 7 wires form a $\pm2°$ stereo angle with respect to the beam direction, while for superlayers 2, 4, 6 and 8 wires are oriented along the beam direction. The measured momentum resolution is $\sigma(p_T)/p_T \sim 0.15\% p_T/(\text{GeV}/c)$. Muon detectors consist of multi-layer drift chambers located around the outside of the calorimeters [7]. The central muon system covers a range in pseudorapidity of $|\eta| < 0.6$. The central muon extension extends the pseudorapidity range to $0.6 < |\eta| < 1.0$.

Data are selected with a three-level trigger system. The Level 1 portion of the dimuon trigger uses the extremely fast tracker [8], providing a coarse track reconstruction based on fast digitization of drift chamber signals. Only tracks with a measured transverse momentum larger than 1.5 GeV/c are considered further. Two such tracks, matched to distinct hits in the muon systems, are required to pass the Level 1 dimuon trigger. No additional requirements are made at Level 2. At Level 3, a detailed reconstruction is performed and opposite sign dimuon events with an invariant mass in the range $2.7-4.0$ GeV/c^2 are accepted and written to tape. Stored events are reconstructed using the full set of calibrations.

The following b hadron decay modes are reconstructed: $B^+ \to J/\psi K^+$, $B^0 \to J/\psi K^{*0}$, $B_s^0 \to J/\psi\phi$, $B^0 \to$ $J/\psi K_S^0$ and $\Lambda_b^0 \to J/\psi\Lambda^0$. The daughter particles are reconstructed in the decay modes $K^{*0} \to K^+\pi^-$, $\phi \to K^+K^-$, $K_S^0 \to \pi^+\pi^-$ and $\Lambda^0 \to p\pi^-$. Charge conjugate modes are included implicitly. To reconstruct a given final state we try all possible combinations of particle hypotheses, since hadronic particle identification capabilities are limited. For a given particle hypothesis tracks are corrected for energy loss with the corresponding mass assigned to the track [9]. The correction procedure [10] makes use of the material information in a GEANT [11] description of the CDF detector. Material is integrated only at radii larger than that of the reconstructed decay vertex of long-lived K_S^0 and Λ^0 particles. High track quality is ensured by requiring at least 20 axial and 16 stereo hits in the COT. To ensure a precise measurement of the b hadron decay vertex, only tracks with at least 3 axial SVX hits are considered. The SVX hit requirement is not applied to the daughter tracks from K_S^0 and Λ^0 which tend to decay outside the silicon tracker. A muon is reconstructed from tracks matched to track stubs in the muon chambers.

The mass reconstruction begins by constraining the two triggered, oppositely charged muons to a common vertex. Candidates with a resulting dimuon mass within 80 MeV/c^2 of the world average J/ψ mass [12] are selected. A p_T threshold of 400 MeV/c is required on all tracks, except Λ^0 daughters, for which all available tracks are used. A uniform threshold of 2 GeV/c is imposed on the momentum transverse to the beam direction of K^+, K^{*0} and ϕ candidates. Mass windows of 80 MeV/c^2, 10 MeV/c^2 and 40 MeV/c^2 around the world average masses [12] are required to select K^{*0}, ϕ and K_S^0, respectively. Combinations with a $p\pi$ mass between 1.10 GeV/c^2 and 1.13 GeV/c^2 are selected as Λ^0 candidates. The K_S^0 and Λ^0 flight directions are reconstructed as the vector connecting the J/ψ and the K_S^0 or Λ^0 vertices. We require the K_S^0 and Λ^0 momentum vectors to be within 0.25° and 0.57° of their flight direction, respectively. A cut on the b hadron transverse momentum $p_T \geq 6.5$ GeV/c is applied. For b hadrons, $c\tau$ is in the range $\sim 400-500$ μm, where τ is the proper lifetime. In order to reduce background, the 2-dimensional decay length of the b hadron, L_{xy}, defined as $L_{xy} = \frac{\vec{X}\cdot\vec{p}_T}{|\vec{p}_T|}$, is required to exceed 100 μm, where $\vec{X}$ is the vector between the production vertex and the decay vertex of the b hadron.

To calibrate the momentum scale of the CDF tracking system, three values must be determined: the energy lost by a track when passing through the material in the inner detector, the radius of the tracker (for the track curvature measurement) and the strength of the magnetic field (for the track curvature-to-momentum conversion). The effect of the tracker radius is indistinguishable from the magnetic field strength in the calibration, so we neglect the tracker radius and describe the procedure in terms of
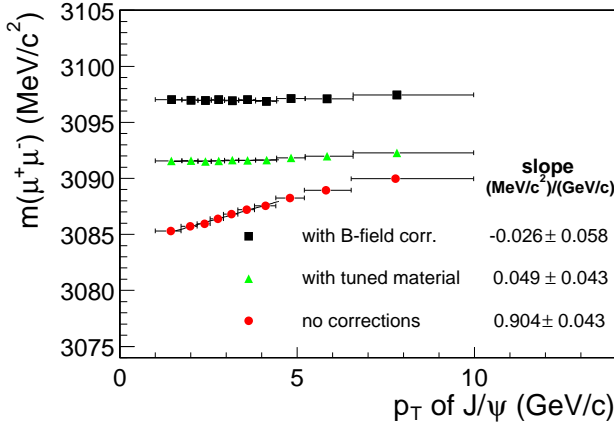
FIG. 1: The reconstructed mass of dimuons from J/ψ decays, as a function of transverse momentum. The three lines represent various stages of corrections: the solid circles indicate no correction, the triangles add the material tuning and the squares show all corrections including the magnetic field scale.

a magnetic field calibration. We use a sample of over 1 million, inclusive $J/\psi \to \mu\mu$ decays to calibrate the track energy loss and magnetic field. An underestimate of the material results in undercorrected energy loss and introduces a dependence of the reconstructed dimuon mass on p_T. The p_T dependence is a signature for inadequate material assessment, as an incorrect value of the magnetic field produces a shift in invariant mass independent of the p_T of the reconstructed particle. The first calibration step tunes the amount of material to remove the momentum dependence. Next the magnetic field is scaled so that the reconstructed $J/\psi \to \mu\mu$ mass agrees with the world average. The effect of the calibration steps on the momentum dependence of the dimuon mass is illustrated in Figure 1. Final state radiation in the decay of the J/ψ leads to an asymmetry in the otherwise Gaussian distribution of the measured dimuon invariant mass. We use a Monte Carlo simulation to correct the resulting bias in bins of J/ψ p_T during calibration.

After reconstruction of candidates the mass is extracted using an unbinned log-likelihood fit, with the signal distribution modeled as a Gaussian. The shape of the background is investigated using an inclusive Monte Carlo sample of b hadron decays. A detailed detector simulation based on GEANT is used. The $B^+ \to J/\psi\,K^+$ sample contains significant contributions of partially reconstructed $B^0 \to J/\psi K^{*0} \to \mu^+\mu^- K^+\pi^-$ and misreconstructed $B^+ \to J/\psi\,\pi^+$ decays, which are modeled in the background probability distribution function. Partially reconstructed $B^0 \to J/\psi K^{*0} \to \mu^+\mu^- K^+\pi^-$ decays populate the left shoulder in Figure 2a). Events from $B^+ \to J/\psi\,\pi^+$ decays appear on the right side of the signal peak. The misreconstruction of $K^{*0} \to K^+\pi^-$ due to swapped track assignment of K and π is taken

into account for $B^0 \to J/\psi\ K^{*0}$ decays. No significant contributions are found for the other decay modes. Comparisons between data and fits are shown in Figure 2.

The systematic uncertainties are summarized in Tables I and II. The largest systematic uncertainties originate from the momentum scale and tracker alignment. Deviations from the well-measured world averages in the $\psi' \to \mu^+\mu^-$, $\psi' \to \mu^+\mu^-\pi^+\pi^-$ and $\Upsilon \to \mu^+\mu^-$ high statistics samples are used to determine the uncertainty of the momentum scale. The observed deviations, scaled by the Q-value of the respective decay, provide an estimate of the systematic uncertainty. The second uncertainty of importance originates from the relative alignment of SVX and COT. It is evaluated by comparing mass measurements using the combined tracker information to those using the COT information alone. False curvature arises from tracker misalignments and results in a curvature offset. The net observed effect is an increase in momentum for negatively charged tracks and a decrease for positively charged tracks. False curvature effects cancel, to first order, in charge symmetric samples. We derive a parametric correction to remove the charge dependence and use the mass shift due to this correction as a measure of the systematic error. Uncertainties due to the vertex fit are evaluated using different mass and pointing constraints in the fit. A correlation between fluctuations in measured curvature and reconstructed vertex position is the source of the resolution bias uncertainty. Background systematics are determined by varying the background description. In the B^+ case, the mass shift due to inclusion and exclusion of the misreconstructed $B^+ \to J/\psi\pi^+$ is assigned as systematic uncertainty. In the B^0 case, the systematic uncertainty is derived by varying the amount of the reflection contribution within 1σ of expectation.

We obtain the following results:

$$
\begin{aligned}
m(B^+) &= 5279.10 \pm 0.41\,_{(stat)} \pm 0.36\,_{(sys)}\ \text{MeV}/c^2, \\
m(B^0) &= 5279.63 \pm 0.53\,_{(stat)} \pm 0.33\,_{(sys)}\ \text{MeV}/c^2, \\
m(B_s^0) &= 5366.01 \pm 0.73\,_{(stat)} \pm 0.33\,_{(sys)}\ \text{MeV}/c^2, \\
m(\Lambda_b^0) &= 5619.7 \pm 1.2\,_{(stat)} \pm 1.2\,_{(sys)}\ \text{MeV}/c^2.
\end{aligned}
$$

These results are in agreement with the current world averages: $m(B^+) = 5279.0 \pm 0.5\ \text{MeV}/c^2$, $m(B^0) = 5279.4 \pm 0.5\ \text{MeV}/c^2$ and $m(B_s^0) = 5369.6 \pm 2.4\ \text{MeV}/c^2$ [13]. Our new Λ_b^0 mass measurement agrees with two of the three previous measurements and is in excellent agreement with CDF's Run I measurement [14, 15, 16]. The achieved precision is better than the current world average of $m(\Lambda_b^0) = 5624 \pm 9\ \text{MeV}/c^2$ [13].

For the mass differences, most systematic uncertainties cancel. The momentum scale uncertainty is scaled down to the size of the mass difference. The remaining systematic uncertainty originates from differences in the fit models. We minimize systematic effects in $m(\Lambda_b^0) - m(B^0)$ by using the $B^0 \to J/\psi K_S^0$ decay mode, which is topologically similar to $\Lambda_b^0 \to J/\psi\Lambda^0$, and where we measure
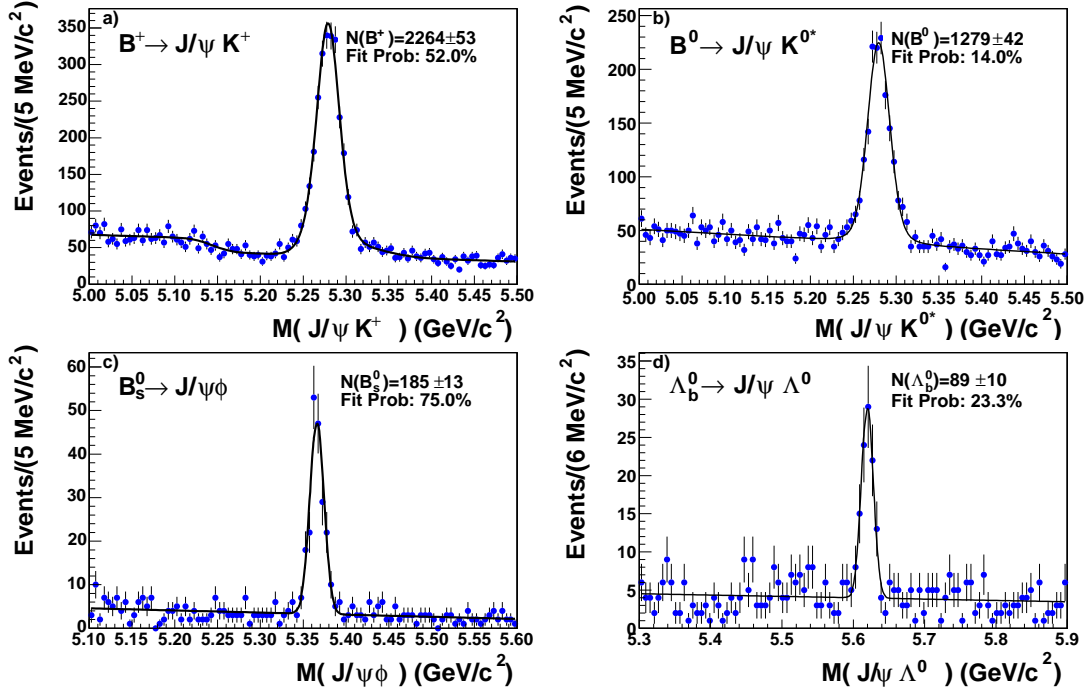
FIG. 2: The invariant mass distribution for $J/\psi\ K^+$, $J/\psi\ K^{0*}$, $J/\psi\ \phi$ and $J/\psi\ \Lambda^0$ candidates. The results of the log-likelihood fits are superimposed. The fit probability obtained from a χ^2 test is shown.

TABLE I: Summary of systematic uncertainties for the B meson mass measurements in MeV/c^2.

Source	$B^0 \to J/\psi K^{*0}$	$B^{\pm} \to J/\psi K^{\pm}$	$B_s^0 \to J/\psi\phi$
Tracking			
Momentum scale	0.20	0.22	0.20
Alignment	0.18	0.18^a	0.18^a
False Curvature	0.02^b	0.02	0.02^b
Vertex Fitting	0.10	0.10^a	0.10^a
Resolution bias	0.13	0.13	0.13
Bkg Systematics			
K-π swap in K^{*0}	0.06	—	—
$J/\psi\pi$ contamin.	—	0.13	—
Total Uncertainty	0.33	0.36	0.33

^{a}from B^0
^{b}from $B^{\pm}$

$m(B^0) = 5280.46 \pm 0.63\ _{(stat)}$, in agreement with the more precise mass determination from the $B^0 \to J/\psi K^{*0}$ decay mode. The uncertainties are summarized in Table III. We obtained the following results for the mass differences:

$$m(B^{\pm}) - m(B^0) = -0.53 \pm 0.67 \pm 0.14\ \text{MeV}/c^2,$$
$$m(B_s^0) - m(B^0) = 86.38 \pm 0.90 \pm 0.06\ \text{MeV}/c^2,$$
$$m(\Lambda_b^0) - m(B^0) = 339.2 \pm 1.4 \pm 0.1\ \text{MeV}/c^2.$$

These are the most precise measurements of $m(B_s^0) - m(B^0)$ and $m(\Lambda_b^0) - m(B^0)$ to date.

We thank the Fermilab staff and the technical staffs

TABLE II: Summary of systematic uncertainties for the Λ_b^0 mass measurement in MeV/c^2. The high statistics B^0 values have been used for the Λ_b^0 systematics.

Source	$B^0 \to J/\psi K_S^0$	$\Lambda_b^0 \to J/\psi\Lambda^0$
Tracking		
Momentum scale	0.2	0.2
Alignment	1.0	1.0^a
Vertex Fitting	0.7	0.7^a
Total uncertainty	1.2	1.2

^{a}from $B^0 \to J/\psi K_S^0$

TABLE III: Summary of systematic uncertainties for the b hadron mass differences in MeV/c^2.

mass difference	mom. scale	fit model	total uncert.
$m(B^{\pm})$ - $m(B^0)$	0.00	0.14	0.14
$m(B_s^0)$ - $m(B^0)$	0.01	0.06	0.06
$m(B_s^0)$ - $m(B^{\pm})$	0.01	0.13	0.13
$m(\Lambda_b^0)$ - $m(B^0)$	0.05	-	0.05

[1] R. Ellis, W. J. Sterling and B. R. Webber, *QCD and Collider Physics* (Cambridge University Press, 1996).

[2] S. Herb *et al.*, Phys. Rev. Lett. **39**, 252 (1977).
[3] C. Davies *et al.*, Phys. Rev. Lett. **92**, 022001 (2004).
[4] D. Acosta *et al.*, Phys. Rev. **D71**, 032001 (2005).
[5] A. Sill *et al.*, Nucl. Instrum. Meth. **A447**, 1 (2000).
[6] T. Affolder *et al.*, Nucl. Instrum. Meth. **A526**, 249 (2004).
[7] G. Ascoli *et al.*, Nucl. Instrum. Meth. **A268**, 33 (1988).
[8] E. J. Thomson *et al.*, IEEE Trans. Nucl. Sci. **49**, 1063 (2002).
[9] D. Acosta *et al.*, Phys. Rev. **D68**, 072004 (2003).
[10] A. Korn, Ph.D. thesis, Massachusetts Institute of Technology (2004).
[11] R. Brun *et al.*, CERN-DD-78-2-REV (unpublished).
[12] D. Groom *et al.* (PDG), Eur. Phys. Jour. **C15** (2000).
[13] S. Eidelman *et al.*, Phys. Lett. **B592** (2004).
[14] F. Abe *et al.*, Phys. Rev. **D55**, 1142 (1997).
[15] D. Buskulic *et al.*, Phys. Lett. **B380**, 442 (1996).
[16] P. Abreu *et al.*, Phys. Lett. **B374**, 351 (1996).